Journal of http://www.satursonpublishing.com/
Research in Multidisciplinary Methods and Applications
ISSN 2957-3920 (Online) ISSN 3007-7060 (Print)
Volume 4, Issue 2, February 2025

The Numerical Solution of Fractional Convection-Diffusion Problems Using a Second-Order Finite Volume Method

Ning Wang, Chao Lang*

School of Applied Science, Beijing Information Science & Technology University, Beijing, 100192, China

*Corresponding to: Chao Lang

Abstract. The time second-order characteristic finite volume method is proposed for solving the one-dimensional Riemann-Liouville space fractional convection-diffusion equation. To be specific, by employing the Euler-Lagrange integration approach, the fractional convection-diffusion equation is transformed into a parabolic-like equation, simplifying its numerical treatment. To achieve a high level of time accuracy, the second-order Runge-Kutta method is applied to solve the characteristic line equation, while the Crank-Nicholson implicit scheme is employed to handle the discretized equations efficiently. Furthermore, the parabolic-like equation is discretized utilizing piecewise linear finite elements to ensure the spatial accuracy. Then, a detailed analysis of the coefficient matrix for iterative equation reveals favorable numerical properties that enhance the stability and convergence of the proposed scheme. Numerical examples are given to verify the convergence order of our scheme is $O(h^{1+\alpha})$ in space step and $O(\tau^2)$ in time step. The results demonstrate the potential of the proposed method as a powerful and effective tool for solving complex fractional convection-diffusion problems in scientific and engineering applications.

Keywords: Riemann-Liouville; Convection-Diffusion Equation; Characteristic Finite Volume Method; Second-Order.

1 INTRODUCTION

In recent years, the theory of fractional calculus has developed rapidly, and the research on its related properties has become more and more important. As a non-local operator, the fractional differential operator needs to depend on the time nodes before and after its time calculation, and it is also closely related to the length calculation in space. Thus, it is this property with memory effect that makes it possible to describe a series of complex dynamic changes in real life more accurately. Because of this, the fractional calculus equations defined by fractional differential operators is widely used in physics, chemistry, biology and many other disciplines [1-7].

There are three common definitions of fractional derivatives: Riemann-Liouville definition, Grunwald-Letnikov definition and Caputo definitions, they are equivalent to each other under certain conditions. Accurate numerical computation of fractional convection-diffusion problems is challenging sexual task. Especially for problems where advection dominates diffusion, and where advective agitation can exacerbate concentration gradients. Traditional numerical methods often encounter problems of unphysical oscillations and excessive numerical diffusion, and these methods cannot guarantee mass conservation, but this property is required for many practical mathematical model applications. Considering the difficulty of finding the analytical solutions of the fractional differential equation (FDE), there had been many effective methods developed for solving the FDEs, such as finite difference methods [8-12], finite element methods [13-15], finite volume methods [16-19] and so on.

Since the finite volume method has local conservation, it is more suitable for modeling conservative partial differential equations. Pan et al. (2017) [20] presented a fast preconditioned iterative finite volume method for solving steady-state space-fractional diffusion equations. Fu et al. (2019) [21] proposed a time second-order finite volume method for solving unsteady space-fractional diffusion equations by Crank-Nicholson scheme where the stability and convergence were proved in L^2 – norm. Zhang et al. (2005) [22] proposed the finite volume method to solve the FADE, where the spatial derivative of the dispersion term was fractional, but the scheme produced numerical oscillations for the transport-dominated diffusive systems.

Journal of http://www.satursonpublishing.com/
Research in Multidisciplinary Methods and Applications
ISSN 2957-3920 (Online) ISSN 3007-7060 (Print)
Volume 4, Issue 2, February 2025

It was well known that the characteristic methods [23] can significantly reduce the truncation errors in time and allow for larger time steps. Wang and Wang (2011) [24] proposed a fast characteristic finite difference method for one-dimensional fractional transient convection-diffusion equations based on fast Fourier transformation and the scheme didn't preserve local mass. Rui and Tabata (2010) [25] developed a mass-conservative characteristic finite element scheme for solving convection-diffusion problems. Colella and Woodwar (1984) [26] developed a piecewise parabolic method (PPM) for solving one-dimensional advection equations. While the method used the parabola interpolation at the previous level, the local mass conservation for the advection problems can be ensured. Further, by introducing the conservative interpolation and the continuous discrete fluxes [27-29] proposed the time second-order characteristic finite difference method and finite volume method solving high-dimensional advection-diffusion equations and atmospheric pollution advection-diffusion problems. The papers [30, 31] proposed the Eulerian-Lagrangian localized adjoint method, which provided the desired local conservation where local conservation was essential for some physical problems. Liang et al. (2017) [32] developed a fractional step ELLAM approach to high-dimensional convection-diffusion equation with forward particle tracking. Until now, there was no work on time second-order characteristic finite volume for solving the space-fractional convection-diffusion equation.

In this paper, we propose a time second-order characteristic finite volume method for solving the one-dimensional Riemann-Liouville space fractional convection-diffusion equation. By the Euler-Lagrange integration technique, we convert the convection-diffusion equation into the parabolic-like equation. Then, the second-order Runge-Kutta method is applied to solve the characteristic line equation while the Crank-Nicholson implicit scheme is used to solve the equations. The equation is discretized by using piecewise linear elements. The properties of the coefficient matrix of the iterative equation are analyzed. Numerical examples are given to verify the convergence order of our scheme is $1+\alpha$ -order in space step and second-order in time step.

The structure of this paper is organized as follows, Firstly, the mathematical model and scheme is considered. Then, the properties of the iterative matrix and error estimation are given. Finally, some numerical examples are tested to verify the spatial and time convergence order.

2 Modeling and Scheme

The space-fractional convection-diffusion equations with an anomalous diffusion of order $0<\alpha\le 1$ in the divergence form are studied as

$$\begin{cases}\dfrac{\partial u}{\partial t}+\dfrac{\partial (Vu)}{\partial x}-\dfrac{\partial}{\partial x}\left(K\left(\gamma\dfrac{\partial^{1-\alpha}u}{\partial x^{1-\alpha}}-(1-\gamma)\dfrac{\partial^{1-\alpha}u}{\partial(-x)^{1-\alpha}}\right)\right)=f(x,t),\ x\in[a,b],\\ u(x,0)=u_0(x),\ x\in[a,b],\\ u(a,t)=0,\ 0\leqslant t\leqslant T,\\ u(b,t)=0,\ 0\leqslant t\leqslant T,\end{cases} \tag{1}$$

where $V(a,\ t)=V(b,\ t)=0$. $\dfrac{\partial^{1-\alpha}u}{\partial x^{1-\alpha}}$ and $\dfrac{\partial^{1-\alpha}u}{\partial(-x)^{1-\alpha}}$ are utilized to denote the left and right Riemann-Liouville fractional derivatives as:

$$\frac{\partial^{1-\alpha}u}{\partial x^{1-\alpha}}=\frac{1}{\Gamma(\alpha)}\frac{\partial}{\partial x}\int_a^x(x-s)^{\alpha-1}u(s)\mathrm{d}s,\quad \frac{\partial^{1-\alpha}u}{\partial(-x)^{1-\alpha}}=-\frac{1}{\Gamma(\alpha)}\frac{\partial}{\partial x}\int_x^b(s-x)^{\alpha-1}u(s)\mathrm{d}s. \tag{2}$$

Let $q(x,t)=K\left(\gamma\dfrac{\partial^{1-\alpha}u}{\partial x^{1-\alpha}}-(1-\gamma)\dfrac{\partial^{1-\alpha}u}{\partial(-x)^{1-\alpha}}\right)$. Then, equation (1) can be rewritten into

$$\begin{cases}\dfrac{\partial u}{\partial t}+\dfrac{\partial (Vu)}{\partial x}-\dfrac{\partial q}{\partial x}=f(x,t),\\ u(x,0)=u_0(x),\ u(a,t)=0,\ u(b,t)=0.\end{cases} \tag{3}$$

The characteristic curve $X(\tau;x,t^{n+1})$ from the point (x,t^{n+1}) satisfies the following relations over the time interval $t\in(t^n,t^{n+1}]$, i.e.,

$$\frac{\mathrm{d}X(\tau;x,t^{n+1})}{\mathrm{d}\tau}=V(X(\tau;x,t^{n+1}),\tau), \tag{4}$$

where τ is the characteristic direction at the time interval $[t^n,t^{n+1}]$ and $X(t^{n+1};x,t^{n+1})=x$. Now, we integrate $\dfrac{\partial u}{\partial t}$ with respect to x over $[x_1,x_2]$ and use Leibniz' rule, it leads to

$$\begin{aligned}\frac{\mathrm{d}}{\mathrm{d}t}\int_{x_1}^{x_2}u(x,t)\,\mathrm{d}x&=\int_{x_1}^{x_2}\frac{\partial u(x,t)}{\partial t}\,\mathrm{d}x+u(x_2,t)\frac{\mathrm{d}x_2}{\mathrm{d}t}-u(x_1,t)\frac{\mathrm{d}x_1}{\mathrm{d}t}\\&=\int_{x_1}^{x_2}\frac{\partial u(x,t)}{\partial t}\,\mathrm{d}x+u(x_2,t)V(x_2,t)-u(x_1,t)V(x_1,t)\\&=\int_{x_1}^{x_2}\frac{\partial u(x,t)}{\partial t}\,\mathrm{d}x+\int_{x_1}^{x_2}\frac{\partial V(x,t)u(x,t)}{\partial x}\,\mathrm{d}x.\end{aligned} \tag{5}$$

Further, we can have that

$$\frac{\mathrm{d}}{\mathrm{d}t}\int_{x_1}^{x_2}u(x,t)\mathrm{d}x\mathrm{d}t-\int_{x_1}^{x_2}\frac{\partial q}{\partial x}\mathrm{d}x\mathrm{d}t=\int_{x_1}^{x_2}f\,\mathrm{d}x\mathrm{d}t. \tag{6}$$

Journal of http://www.satursonpublishing.com/
Research in Multidisciplinary Methods and Applications
ISSN 2957-3920 (Online) ISSN 3007-7060 (Print)
Volume 4, Issue 2, February 2025

The uniform conforming mesh on domain $[a,b]\times[0,T]$ is defined as $\Delta x=\frac{b-a}{N}$ and $\Delta t=\frac{T}{M}$. The staggered grid nodes $\{x_i\}$ and $\{x_{i+1/2}\}$ are set as

$$x_i=a+i\Delta x,\quad i=0,1,\cdots,N,\quad x_{i+1/2}=a+(i+1/2)\Delta x,\quad i=0,1,\cdots,N-1. \tag{7}$$

Integrating (6) over $[t^n,t^{n+1}]$, we can obtain that

$$\int_{t^n}^{t^{n+1}}\frac{\mathrm{d}}{\mathrm{d}t}\int_{x_1}^{x_2}u\mathrm{d}x\mathrm{d}t-\int_{t^n}^{t^{n+1}}\int_{x_1}^{x_2}\frac{\partial q}{\partial x}\mathrm{d}x\mathrm{d}t=\int_{t^n}^{t^{n+1}}\int_{x_1}^{x_2}f\mathrm{d}x\mathrm{d}t. \tag{8}$$

Let $x_1(t^{n+1})=x_{i-1/2}$, $x_2(t^{n+1})=x_{i+1/2}$ and approximate (4) by using second-order Runge-Kutta formula, we then get

$$\overline{x}_{i-1/2}=x_{i-1/2}-\widetilde{V}_{i-1/2}^{n+1/2}\Delta t,\quad \overline{x}_{i+1/2}=x_{i+1/2}-\widetilde{V}_{i+1/2}^{n+1/2}\Delta t, \tag{9}$$

where

$$\widetilde{V}_{i-1/2}^{n+1/2}=\frac{1}{2}[V(x_{i-1/2},t^{n+1})+V(x_{i-1/2}-V(x_{i-1/2},t^{n+1})\Delta t,t^n)].$$

Averaging the diffusion and the source terms along the characteristic line, it follows that

$$\int_{x_1(t^{n+1})}^{x_2(t^{n+1})}u^{n+1}\mathrm{d}x-\int_{x_1(t^n)}^{x_2(t^n)}u^n\mathrm{d}x-\frac{\Delta t}{2}\left(\int_{x_1(t^{n+1})}^{x_2(t^{n+1})}\frac{\partial q^{n+1}}{\partial x}+\int_{x_1(t^n)}^{x_2(t^n)}\frac{\partial q^n}{\partial x}\right)\mathrm{d}x$$
$$=\frac{\Delta t}{2}\left(\int_{x_1(t^{n+1})}^{x_2(t^{n+1})}f^{n+1}+\int_{x_1(t^n)}^{x_2(t^n)}f^n\right)\mathrm{d}x. \tag{10}$$

Substituting (9) into (10), it leads to

$$\int_{x_{i-1/2}}^{x_{i+1/2}}u^{n+1}\mathrm{d}x-\frac{\Delta t}{2}\left(\int_{x_{i-1/2}}^{x_{i+1/2}}\frac{\partial q^{n+1}}{\partial x}\mathrm{d}x+\int_{\overline{x}_{i-1/2}}^{\overline{x}_{i+1/2}}\frac{\partial q^n}{\partial x}\mathrm{d}x\right)=\int_{\overline{x}_{i-1/2}}^{\overline{x}_{i+1/2}}u^n\mathrm{d}x+\frac{\Delta t}{2}\left(\int_{x_{i-1/2}}^{x_{i+1/2}}f^{n+1}\mathrm{d}x+\int_{\overline{x}_{i-1/2}}^{\overline{x}_{i+1/2}}f^n\mathrm{d}x\right). \tag{11}$$

In this study, the finite volume method is used to solve equation (11) effectively. The specific implementation process will be introduced in the next subsection.

Finite Volume Method

Let S_0^N be the space of continuous and piecewise linear functions with respect to the spatial partition, which vanishes at the boundary, and $\varphi_j(x)$ is the nodal linear basis function such that

$$\varphi_j(x)=\begin{cases}(x-x_{j-1})/\Delta x, & x\in[x_{j-1},x_j],\\ (x_{j+1}-x)/\Delta x, & x\in[x_j,x_{j+1}],\ j=1,\cdots,N-1.\\ 0 & \text{else.}\end{cases} \tag{12}$$

Let $u_h^{n+1}(x)=\sum_{j=1}^{N-1}u_j^{n+1}\varphi_j(x)$ be the numerical approximation to the exact solution of (11), we can have that

$$\sum_{j=1}^{N}u_j^{n+1}\int_{x_{i-1/2}}^{x_{i+1/2}}\varphi_j(x)\mathrm{d}x-\frac{\Delta tK}{2}\sum_{j=1}^{N}u_j^{n+1}\left[\mathcal{D}_{x,\gamma}^{\alpha}\varphi_j(x_{i+1/2})-\mathcal{D}_{x,\gamma}^{\alpha}\varphi_j(x_{i-1/2})\right]=\sum_{j=1}^{N}u_j^n\int_{\overline{x}_{i-1/2}}^{\overline{x}_{i+1/2}}\varphi_j(x)\mathrm{d}x$$
$$+\frac{\Delta tK}{2}\sum_{j=1}^{N}u_j^n\left[\mathcal{D}_{x,\gamma}^{\alpha}\varphi_j(\overline{x}_{i+1/2})-\mathcal{D}_{x,\gamma}^{\alpha}\varphi_j(\overline{x}_{i-1/2})\right]+\frac{\Delta t}{2}\left(\int_{x_{i-1/2}}^{x_{i+1/2}}f^{n+1}\mathrm{d}x+\int_{\overline{x}_{i-1/2}}^{\overline{x}_{i+1/2}}f^n\mathrm{d}x\right). \tag{13}$$

where $\mathcal{D}_{\gamma}^{\alpha}:=\gamma\frac{\partial^{1-\alpha}}{\partial x^{1-\alpha}}-(1-\gamma)\frac{\partial^{1-\alpha}}{\partial(-x)^{1-\alpha}}$. By calculating, we can obtain that the follow lemmas.

Lemma 1. For $\varphi_j(x)(j=1,2,\cdots,N-1)$, we can have that

$$\int_{x_{i-1/2}}^{x_{i+1/2}}\varphi_j(x)dx=\frac{\Delta x}{8}\begin{cases}1, & |j-i|=1,\\ 6, & j=i,\\ 0, & \text{else}.\end{cases} \tag{14}$$

and

$$\frac{\partial^{1-\alpha}\varphi_j(x_{i-1/2})}{\partial x^{1-\alpha}}=\frac{1}{\Delta x^{1-\alpha}\Gamma(\alpha+1)}\begin{cases}0, & j>i,\\ s_{i-j}, & j\le i,\end{cases}$$
$$\frac{\partial^{1-\alpha}\varphi_j(x_{i-1/2})}{\partial(-x)^{1-\alpha}}=\frac{1}{\Delta x^{1-\alpha}\Gamma(\alpha+1)}\begin{cases}s_{j-i+1}, & j\ge i-1,\\ 0, & j<i-1,\end{cases}$$
$$\frac{\partial^{1-\alpha}\varphi_j(x_{i+1/2})}{\partial x^{1-\alpha}}=\frac{1}{\Delta x^{1-\alpha}\Gamma(\alpha+1)}\begin{cases}0, & j>i+1,\\ s_{i-j+1}, & j\le i+1,\end{cases}$$
$$\frac{\partial^{1-\alpha}\varphi_j(x_{i+1/2})}{\partial(-x)^{1-\alpha}}=\frac{1}{\Delta x^{1-\alpha}\Gamma(\alpha+1)}\begin{cases}s_{j-i}, & j\ge i,\\ 0, & j<i.\end{cases} \tag{15}$$

Similarly, we have

$$\frac{\partial^{1-\alpha}\varphi_j(\overline{x}_{i-1/2})}{\partial x^{1-\alpha}}=\frac{1}{\Delta x\Gamma(\alpha+1)}\begin{cases}0, & j>i,\\ (\overline{x}_{i-1/2}-x_{j-1})^{\alpha}, & j=i,\\ (\overline{x}_{i-1/2}-x_{j-1})^{\alpha}-2(\overline{x}_{i-1/2}-x_j)^{\alpha}, & j+1=i,\\ (\overline{x}_{i-1/2}-x_{j-1})^{\alpha}-2(\overline{x}_{i-1/2}-x_j)^{\alpha}+(\overline{x}_{i-1/2}-x_{j+1})^{\alpha}, & j+1<i,\end{cases}$$
$$\frac{\partial^{1-\alpha}\varphi_j(\overline{x}_{i-1/2})}{\partial(-x)^{1-\alpha}}=\frac{1}{\Delta x\Gamma(\alpha+1)}\begin{cases}0, & j+1<i,\\ (x_{j+1}-\overline{x}_{i-1/2})^{\alpha}, & j+1=i,\\ (x_{j+1}-\overline{x}_{i-1/2}t)^{\alpha}-2(x_j-\overline{x}_{i-1/2})^{\alpha}, & j=i,\\ (x_{j+1}-\overline{x}_{i-1/2})^{\alpha}-2(x_j-\overline{x}_{i-1/2})^{\alpha}+(x_{j-1}-\overline{x}_{i-1/2})^{\alpha}, & j>i,\end{cases} \tag{16}$$

and

Journal of http://www.satursonpublishing.com/
Research in Multidisciplinary Methods and Applications
ISSN 2957-3920 (Online) ISSN 3007-7060 (Print)
Volume 4, Issue 2, February 2025

$$\frac{\partial^{1-\alpha}\varphi_j(\bar{x}_{i+1/2})}{\partial x^{1-\alpha}}=\frac{1}{\Delta x\Gamma(\alpha+1)}\begin{cases}0, & j-1>i,\\ (\bar{x}_{i+1/2}-x_{j-1})^{\alpha}, & j-1=i,\\ (\bar{x}_{i+1/2}-x_{j-1})^{\alpha}-2(\bar{x}_{i+1/2}-x_j)^{\alpha}, & j=i,\\ (\bar{x}_{i+1/2}-x_{j-1})^{\alpha}-2(\bar{x}_{i+1/2}-x_j)^{\alpha}+(\bar{x}_{i+1/2}-x_{j+1})^{\alpha}, & j<i,\end{cases}$$

$$\frac{\partial^{1-\alpha}\varphi_j(\bar{x}_{i+1/2})}{\partial(-x)^{1-\alpha}}=\frac{1}{\Delta x\Gamma(\alpha+1)}\begin{cases}0, & j<i,\\ (x_{j+1}-\bar{x}_{i+1/2})^{\alpha}, & j=i,\\ (x_{j+1}-\bar{x}_{i+1/2})^{\alpha}-2(x_j-\bar{x}_{i+1/2})^{\alpha}, & j-1=i,\\ (x_{j+1}-\bar{x}_{i+1/2})^{\alpha}-2(x_j-\bar{x}_{i+1/2})^{\alpha}+(x_{j-1}-\bar{x}_{i+1/2})^{\alpha}, & j-1>i,\end{cases} \tag{17}$$

where

$$s_k=\begin{cases}(1/2)^{\alpha} & k=0,\\ (3/2)^{\alpha}-2(1/2)^{\alpha} & k=1,\\ (k+1/2)^{\alpha}-2(k-1/2)^{\alpha}+(k-3/2)^{\alpha} & 2\le k\le N-1.\end{cases} \tag{18}$$

By introducing the following symbol, equation (16) and (17) can be written as

$$\frac{\partial^{1-\alpha}\varphi_j(\bar{x}_{i-1/2})}{\partial x^{1-\alpha}}=\begin{cases}0, & j>i,\\ \tilde{k}_0, & j=i,\\ \tilde{k}_1, & j+1=i,\\ \tilde{k}_{ij}, & j+2\le i,\end{cases}\quad \frac{\partial^{1-\alpha}\varphi_j(\bar{x}_{i-1/2})}{\partial(-x)^{1-\alpha}}=\begin{cases}0, & j+1<i,\\ \hat{k}_0, & j+1=i,\\ \hat{k}_1, & j=i,\\ \hat{k}_{ij}, & j-1\ge i,\end{cases}$$

$$\frac{\partial^{1-\alpha}\varphi_j(\bar{x}_{i+1/2})}{\partial x^{1-\alpha}}=\begin{cases}0, & j-1>i,\\ \tilde{s}_0, & j-1=i,\\ \tilde{s}_1, & j=i,\\ \tilde{s}_{ij}, & j+1\le i,\end{cases}\quad \frac{\partial^{1-\alpha}\varphi_j(\bar{x}_{i+1/2})}{\partial(-x)^{1-\alpha}}=\begin{cases}0, & j<i,\\ \hat{s}_0, & j=i,\\ \hat{s}_1, & j-1=i,\\ \hat{s}_{ij}, & j-2\ge i.\end{cases} \tag{19}$$

Next, we give the matrix format of (13). Let

$$\begin{cases}\mathbf{U}^n=\left[u_1^n,u_2^n,\ldots,u_{N-1}^n\right]^{\mathrm{T}},\\ \mathbf{F}^n=\left[\bar{f}_1^n,\bar{f}_2^n\ldots,\bar{f}_{N-1}^n\right]^{\mathrm{T}},\\ \mathbf{U}^{n+1}=\left[u_1^{n+1},u_2^{n+1},\ldots,u_{N-1}^{n+1}\right]^{\mathrm{T}},\\ \mathbf{F}^{n+1}=\left[\hat{f}_1^{n+1},\hat{f}_2^{n+1}\ldots,\hat{f}_{N-1}^{n+1}\right]^{\mathrm{T}},\end{cases} \tag{20}$$

where $\bar{f}_i^n=\frac{1}{\Delta x}\int_{\bar{x}_{i-1/2}}^{\bar{x}_{i+1/2}}f(x,t^n)\mathrm{d}x$ and $\hat{f}_i^{n+1}=\frac{1}{\Delta x}\int_{x_{i-1/2}}^{x_{i+1/2}}f(x,t^{n+1})\mathrm{d}x.$

Define the mass matrix $\mathbf{A}$ as

$$\mathbf{A}=\frac{1}{8}\begin{bmatrix}6&1&0&\cdots&0&0\\1&6&1&\ddots&\ddots&0\\\vdots&1&6&\ddots&\ddots&0\\\vdots&\ddots&\ddots&\ddots&\ddots&0\\0&\ddots&\ddots&\ddots&6&1\\0&0&\ldots&\ldots&1&6\end{bmatrix}, \tag{21}$$

Then, the stiffness matrix $\mathbf{B}=\gamma\mathbf{T}+(1-\gamma)\mathbf{T}^{\mathrm{T}}$ with

$$\mathbf{T}=\begin{bmatrix}s_0-s_1&-s_0&0&\cdots&0&0\\s_1-s_2&s_0-s_1&-s_0&\ddots&\ddots&0\\\vdots&s_1-s_2&s_0-s_1&\ddots&\ddots&\vdots\\\vdots&\ddots&\ddots&\ddots&\ddots&0\\s_{N-3}-s_{N-2}&\ddots&\ddots&\ddots&s_0-s_1&-s_0\\s_{N-2}-s_{N-1}&s_{N-3}-s_{N-2}&\cdots&\cdots&s_1-s_2&s_0-s_1\end{bmatrix}, \tag{22}$$

and $\tilde{\mathbf{B}}=\gamma\mathbf{P}+(1-\gamma)\mathbf{Q}$ with

$$\mathbf{P}=\begin{bmatrix}\tilde{k}_0-\tilde{s}_1&-\tilde{s}_0&0&\cdots&0&0\\\tilde{k}_1-\tilde{s}_2&\tilde{k}_0-\tilde{s}_1&-\tilde{s}_0&\ddots&\ddots&0\\\vdots&\tilde{k}_1-\tilde{s}_2&\tilde{k}_0-\tilde{s}_1&\ddots&\ddots&\vdots\\\vdots&\ddots&\ddots&\ddots&\ddots&0\\\tilde{k}_{N-2,1}-\tilde{s}_{N-1,1}&\ddots&\ddots&\ddots&\tilde{k}_0-\tilde{s}_1&-\tilde{s}_0\\\tilde{k}_{N-1,1}-\tilde{s}_{N,1}&\tilde{k}_{N-1,2}-\tilde{s}_{N,2}&\cdots&\cdots&\tilde{k}_1-\tilde{s}_2&\tilde{k}_0-\tilde{s}_1\end{bmatrix}, \tag{23}$$

and

$$\mathbf{Q}=\begin{bmatrix}\bar{s}_0-\bar{k}_1&\bar{s}_1-\bar{k}_2&\cdots&\cdots&\bar{s}_{1,N-2}-\bar{k}_{1,N-1}&\bar{s}_{1,N-1}-\bar{k}_{1,N}\\-\bar{k}_0&\bar{s}_0-\bar{k}_1&\bar{s}_1-\bar{k}_2&\ddots&\ddots&\bar{s}_{2,N-1}-\bar{k}_{2,N}\\0&-\bar{k}_0&\bar{s}_0-\bar{k}_1&\ddots&\ddots&\vdots\\\vdots&\ddots&\ddots&\ddots&\ddots&\vdots\\0&\ddots&\ddots&\ddots&\bar{s}_0-\bar{k}_1&\bar{s}_1-\bar{k}_2\\0&0&\cdots&0&-\bar{k}_0&\bar{s}_0-\bar{k}_1\end{bmatrix}. \tag{24}$$

Let $\tilde{\mathbf{A}}(i,j)=\frac{1}{\Delta x}\int_{\bar{x}_{i-1/2}}^{\bar{x}_{i+1/2}}\varphi_j(x)\mathrm{d}x,$ by referring to equation (13), we have that

$$(\mathbf{A}+\eta_1\mathbf{B})\mathbf{U}^{n+1}=(\tilde{\mathbf{A}}+\eta_2\tilde{\mathbf{B}})\mathbf{U}^n+\frac{\tau}{2}(\mathbf{F}^n+\mathbf{F}^{n+1}), \tag{25}$$

where $\eta_1=\frac{K\Delta t}{2\Gamma(\alpha+1)\Delta x^{2-\alpha}}$, $\eta_2=\frac{-K\Delta t}{2\Gamma(\alpha+1)\Delta x^2}$.

Remark 1. Assuming that $|\bar{x}_{i-1/2}-x_{i-1/2}|\le\Delta x/2$, we can have that

Journal of http://www.satursonpublishing.com/
Research in Multidisciplinary Methods and Applications
ISSN 2957-3920 (Online) ISSN 3007-7060 (Print)
Volume 4, Issue 2, February 2025

$$\int_{\bar{x}_{i-1/2}}^{\bar{x}_{i+1/2}} \varphi_j(x) = \frac{1}{\Delta x}\begin{cases} \int_{\bar{x}_{i-1/2}}^{x_i} (x_{j+1}-x)\mathrm{d}x, & j=i-1, \\ \int_{\bar{x}_{i-1/2}}^{x_i} (x-x_{j-1})\mathrm{d}x + \int_{x_i}^{\bar{x}_{i+1/2}} (x_{j+1}-x)\mathrm{d}x, & j=i, \\ \int_{x_i}^{\bar{x}_{i+1/2}} (x-x_{j-1})\mathrm{d}x, & j=i+1, \\ 0, & \text{else.} \end{cases} \tag{26}$$

Thus, we derive that $\widetilde{\mathbf{A}}$ is tri-diagonal matrix.

3 PROPERTIES OF ITERATIVE MATRIX

The Properties Of s_k

For $0<\alpha<1$, define $G(x)$ as

$$G(x)=g(x)-g(x-1),\ x>2, \quad g(x)=(x+\frac{1}{2})^{\alpha}-(x-\frac{1}{2})^{\alpha},\ x\geq 1. \tag{27}$$

Thus, we can have that

$$\sum_{k=2}^{N-1} G(k) = \sum_{k=2}^{N-1}(g(k)-g(k-1)) = g(N-1)-g(1). \tag{28}$$

Further, we can derive that

$$\begin{aligned} g'(x) &= \alpha\left[(x+1/2)^{\alpha-1}-(x-1/2)^{\alpha-1}\right]<0, \\ g''(x) &= \alpha(\alpha-1)\left[(x+1/2)^{\alpha-2}-(x-1/2)^{\alpha-2}\right]>0. \end{aligned} \tag{29}$$

So, we get that

$$G(2)<G(3)<G(4)<\cdots<G(k)<\cdots<0, \tag{30}$$

and $G(0)>0$, $G(1)$ is dependent on α.

Define $\widetilde{G}(x)$ as

$$\widetilde{G}(x)=G(x)-G(x+1), \quad x\geq 2, \tag{31}$$

i.e.,

$$\widetilde{G}(k)=s_k-s_{k+1}, \quad k=2,3,\cdots,N-1. \tag{32}$$

It is not difficult to derive that

$$g'''(x)=\alpha(\alpha-1)(\alpha-2)\left[(x+1/2)^{\alpha-2}-(x-1/2)^{\alpha-2}\right]<0, \tag{33}$$

Thus, it holds that

$$G''(x)=g''(x)-g''(x-1)<0, \quad \widetilde{G}'(x)=G'(x)-G'(x+1)>0, \tag{34}$$

We can prove that

$$\widetilde{G}(2)<\widetilde{G}(3)<\widetilde{G}(4)<\cdots<0. \tag{35}$$

The properties of matrix

Let

$$t_c=[t_0,t_1,\ldots,t_{N-1}]^{\mathrm{T}}, \quad t_r=[t_0,t_{-1},\ldots,t_{1-N}]^{\mathrm{T}}, \tag{36}$$

where

$t_k=\widetilde{G}(k),\ k=0,1,2,\ldots,N-1,\ t_{-1}=-G_0,\ t_{-k}=0,\ k=2,3,\ldots,N-1.$

Lemma 2. For $0<\alpha<1$, $\forall N\in N^+$, $\mathbf{T}$ is strictly diagonally dominant iff $s_1-s_2<0$.

Proof. When $s_1-s_2<0$, it holds that

$$\sum_{k=1}^{N-1}|t_k| = -\sum_{k=1}^{N-1}(s_k-s_{k+1}) = -s_1+s_N, \tag{37}$$

Due to $s_N<0$, it follows that

$$\sum_{k=1}^{N-1}(|t_k|+|t_{-k}|) = s_0-s_1+s_N < s_0-s_1=t_0. \tag{38}$$

We complete the proof. □

Let

$$b_c=[b_0,b_1,\ldots,b_{N-1}]^{\mathrm{T}}, \quad b_r=[b_0,b_{-1},\ldots,b_{1-N}]^{\mathrm{T}}, \tag{39}$$

with

$$\begin{cases} b_0=s_0-s_1, \\ b_1=\gamma(s_1-s_2)-(1-\gamma)s_0, \\ b_{-1}=(1-\gamma)(s_1-s_2)-\gamma s_0, \\ b_k=\gamma(s_k-s_{k+1}),\ k=2,3,\ldots,N-1, \\ b_{-k}=(1-\gamma)(s_k-s_{k+1}),\ k=2,3,\ldots,N-1. \end{cases} \tag{40}$$

When $0<\gamma<1$, by (35), we have that

$$\sum_{k=1}^{N-1}(|b_k|+|b_{-k}|) = |b_1|+|b_{-1}|+\sum_{2}^{N_1}(s_{k+1}-s_k) = |b_1|+|b_{-1}|-s_2+s_N. \tag{41}$$

Lemma 3. When $0<\gamma<1$, $0<\alpha<1$ and $s_1-s_2\leq 0$, $\mathbf{B}$ is strictly diagonally dominant matrix.

Proof. when $s_1-s_2\leq 0$, it follows that

$$b_1\leq 0, \quad b_{-1}\leq 0. \tag{42}$$

Journal of http://www.satursonpublishing.com/
Research in Multidisciplinary Methods and Applications
ISSN 2957-3920 (Online) ISSN 3007-7060 (Print)
Volume 4, Issue 2, February 2025

Further, we can obtain that

$$\sum_{k=1}^{N-1}\left(|b_k|+|b_{-k}|\right)=s_0-s_1+s_N<s_0-s_1=|b_0|. \quad (43)$$

We complete the proof. □

Remark 2. By **Lemma** 3, we can prove that the coefficient matrix $\mathbf{A}+\eta_1\mathbf{B}$ are strictly diagonally dominant and solvability.

4 Error Estimate

4.1 Time Error Estimation

The initial value problem of the first-order ordinary differential equation (4) is studied as

$$\begin{cases}\dfrac{\mathrm{d}x}{\mathrm{d}t}=V(t,x), t\in[0,T],\\ x(0)=x_0.\end{cases} \quad (44)$$

Next, we consider the second-order Runge-Kutta method as

$$\begin{cases}x_{n+1}=x_n+\Delta t\left(c_1K_1+c_2K_2\right),\\ K_1=V\left(t^n,x_n\right),\\ K_2=V\left(t^n+\lambda_2\Delta t,x_n+\mu_{21}\Delta tK_1\right).\end{cases} \quad (45)$$

Here $c_1,c_2,\lambda_2,\mu_{21}$ are all undetermined constants. According to the definition of local truncation error, the local truncation error of this method is

$$T_{n+1}=x\left(t^{n+1}\right)-x\left(t^n\right)-\Delta t\left[c_1V\left(t^n,x_n\right)+c_2V\left(t^n+\lambda_2\Delta t,x_n+\mu_{21}\Delta tV_n\right)\right], \quad (46)$$

where $x_n=x(t^n),V_n=V(t^n,x_n)$. In order to get p-order T_{n+1}, the Taylor expansion of the terms for the above equation should be done at (t^n,x_n) and the expansions are as follows

$$x(t^{n+1})=x_n+\Delta tx_n^{'}+\frac{(\Delta t)^2}{2}x_n^{''}+\frac{(\Delta t)^3}{3!}x_n^{'''}+O\left((\Delta t)^4\right), \quad (47)$$

with

$$\begin{cases}x_n^{'}=V\left(t^n,x_n\right),\\ x_n^{''}=\dfrac{\mathrm{d}}{\mathrm{d}t}V\left(t^n,x\left(t^n\right)\right)=V_t^{'}\left(t^n,x_n\right)+V_x^{'}\left(t_n,x_n\right)V_n,\\ x_n^{'''}=V_{tt}^{''}\left(t^n,x_n\right)+2V_nV_{tx}^{''}\left(t^n,x_n\right)+V_n^2V_{xx}^{''}\left(t_n,x_n\right)+V_x^{'}\left(t^n,x_n\right)\left[V_t^{'}\left(t^n,x_n\right)+V_nV_x^{'}\left(t^n,x_n\right)\right],\end{cases} \quad (48)$$

and

$$V\left(t^n+\lambda_2\Delta t,x_n+\mu_{21}\Delta tV_n\right)=V_n+V_t^{'}\left(t^n,x_n\right)\lambda_2\Delta t+V_x^{'}\left(t^n,x_n\right)\mu_{21}\Delta tV_n+O\left((\Delta t)^2\right). \quad (49)$$

Substituting (47), (48) and (49) into (46), we can have that

$$\begin{aligned}T_{n+1}&=\Delta tV_n+\frac{(\Delta t)^2}{2}\left[V_t^{'}\left(t^n,x_n\right)+V_x^{'}\left(t^n,x_n\right)V_n\right]\\&-\Delta t\left[c_1V_n+c_2\left(V_n+\lambda_2V_t^{'}\left(t^n,x_n\right)\Delta t+\mu_{21}V_x^{'}\left(t^n,x_n\right)V_n\Delta t\right)\right]+O\left((\Delta t)^3\right)\\&=(1-c_1-c_2)V_n\Delta t+\left(\frac{1}{2}-c_2\lambda_2\right)V_t^{'}\left(t^n,x_n\right)(\Delta t)^2+\left(\frac{1}{2}-c_2\mu_{21}\right)V_x^{'}\left(t^n,x_n\right)V_n(\Delta t)^2+O\left((\Delta t)^3\right).\end{aligned} \quad (50)$$

For the scheme (8), namely $a=1/2,c_1=c_2=1/2,\lambda_2=\mu_{21}=1$, by substituting these parameters into equation (50), we can get $T_{n+1}=O\left((\Delta t)^3\right)$. Therefore, it shows that the proposed scheme (13) is second-order accurate in time.

4.2 Space Error Estimation

Define

$$\begin{aligned}{}_a\mathcal{I}_x^{\alpha}g(x)&:=\frac{1}{\Gamma(\alpha)}\int_a^x(x-s)^{\alpha-1}g(s)\mathrm{d}s,\\ {}_x\mathcal{I}_{\mathrm{b}}^{\alpha}g(x)&:=\frac{1}{\Gamma(\alpha)}\int_x^b(s-x)^{\alpha-1}g(s)\mathrm{d}s,\\ \mathcal{D}_{x,\gamma}^{\alpha}&:=\gamma\frac{\partial^{1-\alpha}}{\partial x^{1-\alpha}}-(1-\gamma)\frac{\partial^{1-\alpha}}{\partial(-x)^{1-\alpha}}.\end{aligned} \quad (51)$$

Lemma 4. Let $g(x)\in C[a,b]$, for $0<\alpha<1$, there is a constant C independent of h, satisfy

$${}_a\mathcal{I}_x^{\alpha}g(x)\Big|_{x_{i-1/2}}^{x_{i+1/2}}=Ch^{\alpha},\quad {}_x\mathcal{I}_b^{\alpha}g(x)\Big|_{x_{i-1/2}}^{x_{i+1/2}}=Ch^{\alpha}. \quad (52)$$

Proof. By the definition in (51), we can get that

$$\begin{aligned}{}_a\mathcal{I}_x^{\alpha}g(x)\Big|_{x_{i-1/2}}^{x_{i+1/2}}&=\frac{1}{\Gamma(\alpha)}\int_a^{x_{i-1/2}}g(s)\left(\left(x_{i+1/2}-s\right)^{\alpha-1}-\left(x_{i-1/2}-s\right)^{\alpha-1}\right)\mathrm{d}s\\&+\frac{1}{\Gamma(\alpha)}\int_{x_{i-1/2}}^{x_{i+1/2}}g(s)\left(x_{i+1/2}-s\right)^{\alpha-1}\mathrm{d}s:=I_1+I_2,\end{aligned} \quad (53)$$

If $s\in[a,x_{i-1/2}]$, i.e.,

$$\begin{aligned}|I_1|&\le\frac{\|g\|}{\Gamma(\alpha)}\int_a^{x_i-1/2}\left(x_{i-1/2}-s\right)^{\alpha-1}-\left(x_{i+1/2}-s\right)^{\alpha-1}\mathrm{d}s\\&=\frac{\|g\|}{\Gamma(\alpha+1)}\left(\left(x_{i-1/2}-a\right)^{\alpha}-\left(x_{i+1/2}-a\right)^{\alpha}+\left(x_{i+1/2}-x_{i-1/2}\right)^{\alpha}\right)\le C\|g\|h^{\alpha},\end{aligned} \quad (54)$$

where $\|g\|=\max|g|$. If $s\in[x_{i-1/2},x_{i+1/2}]$,

$$|I_2|\le\frac{\|g\|}{\Gamma(\alpha)}\int_{x_{i-1/2}}^{x_{i+1/2}}\left(x_{i+1/2}-s\right)^{\alpha-1}\mathrm{d}s=\frac{\|g\|}{\Gamma(\alpha+1)}\left(x_{i+1/2}-x_{i-1/2}\right)^{\alpha}\le C\|g\|h^{\alpha}. \quad (55)$$

Journal of http://www.satursonpublishing.com/
Research in Multidisciplinary Methods and Applications
ISSN 2957-3920 (Online) ISSN 3007-7060 (Print)
Volume 4, Issue 2, February 2025

We complete the proof. □

Lemma 5. Define

$$\mathcal{P}_h g(x) := \sum_{i=1}^{N} g(x_i)\varphi_i(x). \tag{56}$$

The spatial truncation error is

$$r^n = K\mathcal{D}_{x,\gamma}^{\alpha}\left(u(x,t_n) - \mathcal{P}_h u(x,t_n)\right), \tag{57}$$

where

$$\left| r^n \right|_{x_{i-1/2}}^{x_{i+1/2}} | \le Ch^{1+\alpha}. \tag{58}$$

5 NUMERICAL EXPERIMENTS

In this section, some numerical examples are given to verify the convergence order of our scheme is of convergent $O(h^{1+\alpha})$ in space and is $O(\tau^2)$ in time. In example 1 and 2, we assume that the domain $[a,b]=[0,1]$ and the total time $T=1$.

Example 1. Take the initial solution $u(x,0)=4x^2(1-x)^2$ and $V(x)=V_0(1-x)x$. The source function is given as

$$f(x,t) = -4\mathrm{e}^{-t}x^2(1-x)^2 + 4V_0\mathrm{e}^{-t}(3x^2(x-1)^2(1-2x)) - 8\mathrm{e}^{-t}K(\gamma\omega(x,\alpha)+(1-\gamma)\omega(1-x,\alpha)), \tag{59}$$

with

$$\omega(\alpha,x) = \frac{x^{\alpha}}{\Gamma(1+\alpha)} - \frac{6x^{1+\alpha}}{\Gamma(2+\alpha)} + \frac{12x^{2+\alpha}}{\Gamma(3+\alpha)}, \tag{60}$$

where $V_0 = 0.1,\ K = 1$. We can solve the exact solution as

$$u(x,t) = 4\mathrm{e}^{-t}x^2(1-x)^2. \tag{61}$$

The convergence order of our scheme is given in Table 1 - Table 2. In Table 1, we take the time step $\Delta t = 1/10000$ and the space $h = 1/10, 1/20, 1/40$ and $1/80$, respectively.

TABLE 1. ERRORS AND ORDERS OF CONVERGENCE IN SPACE FOR EXAMPLE 1.

		h	1/10	1/20	1/40	1/80
$\alpha = 0.1$	$\gamma = 0.0$	e_h	4.4447E-03	1.2397E-03	3.8223E-04	1.3582E-04
		order	-	1.843	1.697	1.499
	$\gamma = 0.5$	e_h	4.0033E-03	9.9995E-04	2.4622E-04	6.0535E-05
		order	-	2.013	2.021	2.024
	$\gamma = 1.0$	e_h	4.4002E-03	1.2232E-03	3.7823E-04	1.3589E-04
		order	-	1.847	1.694	1.477
$\alpha = 0.5$	$\gamma = 0.0$	e_h	7.0972E-03	2.1115E-03	6.3768E-04	1.9716E-04
		order	-	1.749	1.727	1.693
	$\gamma = 0.5$	e_h	2.9837E-03	6.8737E-04	1.5696E-04	3.5858E-05
		order	-	2.118	2.131	2.130
	$\gamma = 1.0$	e_h	7.1700E-03	2.1510E-03	6.5292E-04	2.0284E-04
		order	-	1.737	1.720	1.687
$\alpha = 0.9$	$\gamma = 0.0$	e_h	8.0962E-03	2.2775E-03	5.8661E-04	1.5065E-04

Journal of http://www.satursonpublishing.com/
Research in Multidisciplinary Methods and Applications
ISSN 2957-3920 (Online) ISSN 3007-7060 (Print)
Volume 4, Issue 2, February 2025

		order	-	1.830	1.952	1.966
	$\gamma = 0.5$	e_h	2.0334E-03	4.7468E-04	1.1334E-04	2.7743E-05
		order	-	2.099	2.066	2.030
	$\gamma = 1.0$	e_h	9.5268E-03	2.5969E-03	6.6695E-04	1.7157E-04
		order	-	1.875	1.956	1.964

From Table 1, we can observe that the space convergence order of our scheme tends to $1+\alpha$ when the space fractional order $\alpha = 0.1,\ 0.5$ and 0.9. under the spatial discrete steps h tends to zeros. Meanwhile, it is not difficult to find that the space order tends to second-order when the left and right diffusion weight $\gamma = 0.5$. Moreover, the space convergence order in Example 1 is plotted in Figure 1 as follows.

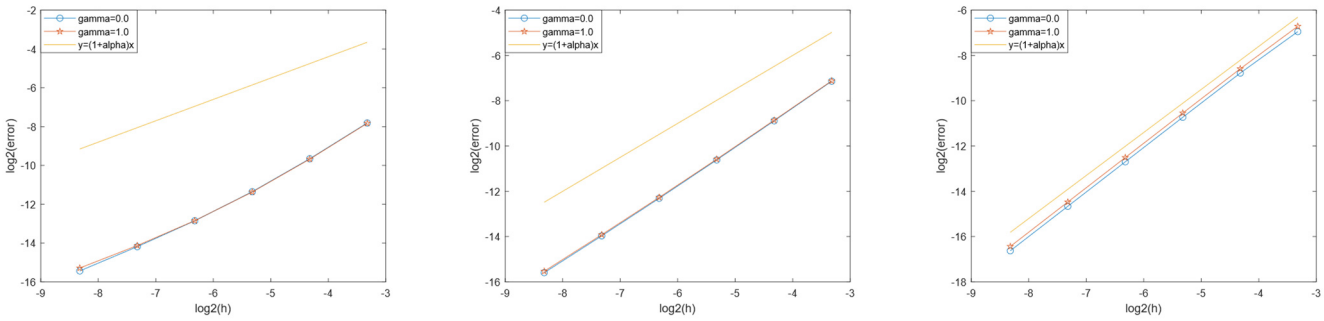

(A) $\alpha = 0.1$ **(B)** $\alpha = 0.5$ **(C)** $\alpha = 0.9$

FIGURE 1. THE PLOT OF SPACE CONVERGENCE ORDER FOR EXAMPLE 1.

From Figure 1, we can clearly see that the spatial convergence order of the proposed scheme is $1+\alpha$. Next, we analyze the time convergence of our scheme.

In Table 2, we take $\Delta t = 0.1h^{(1+\alpha)/2}$ with the space step $h = 1/10,\ 1/20,\ 1/40$. It is easily to see that the proposed scheme is of convergence second-order in time. This conclusion can be found more intuitively in Figure 2.

TABLE 2. ERRORS AND ORDERS OF CONVERGENCE IN TIME FOR EXAMPLE 1.

		h	1/10	1/20	1/40
$\alpha = 0.1$	$\gamma = 0.0$	e_h	2.7462E-03	8.9851E-03	2.8862E-04
		order	-	2.901	2.948
	$\gamma = 0.5$	e_h	2.4248E-03	8.5695E-04	2.7510E-04
		order	-	2.716	2.967

Journal of http://www.satursonpublishing.com/
Research in Multidisciplinary Methods and Applications
ISSN 2957-3920 (Online) ISSN 3007-7060 (Print)
Volume 4, Issue 2, February 2025

	$\gamma = 1.0$	e_h	2.7904E-03	9.0238E-03	3.0414E-04
		order	-	2.886	2.901
$\alpha = 0.5$	$\gamma = 0.0$	e_h	5.7360E-03	1.5033E-03	4.0803E-04
		order	-	2.511	2.445
	$\gamma = 0.5$	e_h	2.2549E-03	5.9792E-04	1.7147E-04
		order	-	2.729	2.361
	$\gamma = 1.0$	e_h	5.7787E-03	1.5195E-03	4.1437E-04
		order	-	2.524	2.456
$\alpha = 0.9$	$\gamma = 0.0$	e_h	6.7922E-03	1.8526E-03	4.7596E-04
		order	-	1.968	2.058
	$\gamma = 0.5$	e_h	1.5378E-03	4.1252E-04	9.0653E-04
		order	-	1.993	2.295
	$\gamma = 1.0$	e_h	8.3507E-03	1.9659E-03	4.4798E-04
		order	-	2.191	2.240

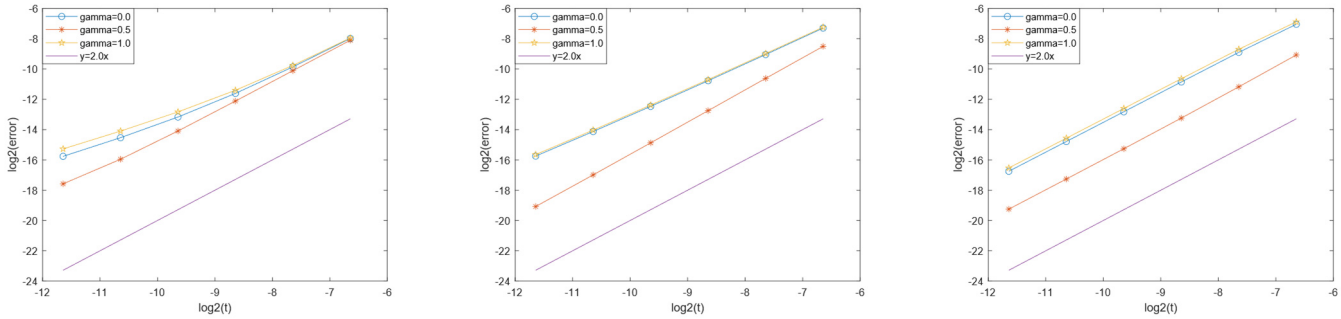

(A) $\alpha = 0.1$ **(B)** $\alpha = 0.5$ **(C)** $\alpha = 0.9$

FIGURE 2. THE PLOT OF TIME CONVERGENCE ORDER FOR EXAMPLE 1.

Example 2. Take the initial solution $u(x,0) = x(1-x)$ and $V(x) = V_0(1-x)^2x^2$. The source function is set as

$$f(x,t) = e^t x(1-x) + V_0 e^t (3x^2(1-x)^2(1-2x)) - e^t K(\gamma P(x,\alpha) + (1-\gamma)P(1-x,\alpha)), \tag{62}$$

with

Journal of http://www.satursonpublishing.com/
Research in Multidisciplinary Methods and Applications
ISSN 2957-3920 (Online) ISSN 3007-7060 (Print)
Volume 4, Issue 2, February 2025

$$P(x,\alpha)=\frac{x^{\alpha-1}}{\Gamma(\alpha)}-\frac{2x^{\alpha}}{\Gamma(1+\alpha)}, \tag{63}$$

$$u(x,t)=\mathrm{e}^{t}x(1-x). \tag{64}$$

Similarly, the computational results are recorded as follows.

where $V_0=0.1,\ K=1.$ The exact solution is solved as

TABLE 3. ERRORS AND ORDERS OF CONVERGENCE IN SPACE FOR EXAMPLE 2.

		h	1/10	1/20	1/40	1/80
$\alpha=0.1$	$\gamma=0.0$	e_h	1.1119E-03	3.0995E-04	9.5591E-05	3.3820E-05
		order	-	1.843	1.697	1.499
	$\gamma=0.5$	e_h	1.0083E-03	2.4989E-04	6.1555E-05	1.5134E-05
		order	-	2.013	2.021	2.024
	$\gamma=1.0$	e_h	1.1001E-03	3.0582E-03	9.4558E-04	3.3974E-05
		order	-	1.847	1.693	1.477
$\alpha=0.5$	$\gamma=0.0$	e_h	1.7743E-03	5.2789E-04	1.5942E-04	4.9290E-05
		order	-	1.749	1.727	1.693
	$\gamma=0.5$	e_h	7.4593E-03	1.7184E-04	3.9242E-05	8.9647E-06
		order	-	2.118	2.131	2.130
	$\gamma=1.0$	e_h	1.7925E-03	5.3776E-04	1.6323E-04	5.0711E-05
		order	-	1.737	1.720	1.687
$\alpha=0.9$	$\gamma=0.0$	e_h	2.0241E-03	5.6940E-03	1.4715E-04	3.7663E-05
		order	-	1.830	1.952	1.966
	$\gamma=0.5$	e_h	5.0837E-04	1.1187E-04	2.8336E-05	6.9352E-06
		order	-	2.099	2.066	2.030
	$\gamma=1.0$	e_h	2.3817E-03	6.4924E-04	1.6737E-04	4.2895E-05
		order	-	1.875	1.956	1.964

Journal of http://www.satursonpublishing.com/
Research in Multidisciplinary Methods and Applications
ISSN 2957-3920 (Online) ISSN 3007-7060 (Print)
Volume 4, Issue 2, February 2025

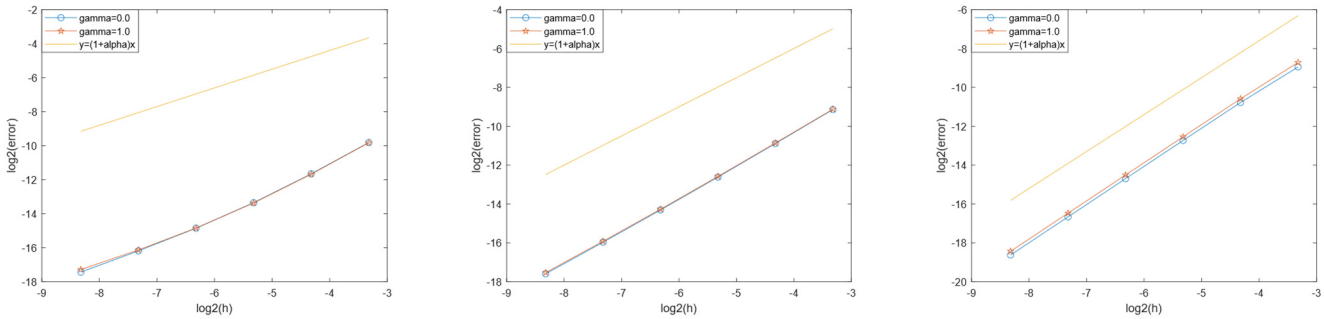

(A) $\alpha = 0.1$ (B) $\alpha = 0.5$ (C) $\alpha = 0.9$

FIGURE 3. THE PLOT OF SPACE CONVERGENCE ORDER FOR EXAMPLE 2.

TABLE 4. ERRORS AND ORDERS OF CONVERGENCE IN TIME FOR EXAMPLE 2.

		h	1/10	1/20	1/40
$\alpha = 0.1$	$\gamma = 0.0$	e_h	6.6856E-03	2.2463E-04	7.2157E-05
		order	-	2.901	2.948
	$\gamma = 0.5$	e_h	6.0621E-04	2.1424E-04	6.8776E-05
		order	-	2.716	2.967
	$\gamma = 1.0$	e_h	6.9762E-04	2.3096E-04	7.6035E-05
		order	-	2.886	2.901
$\alpha = 0.5$	$\gamma = 0.0$	e_h	1.4399E-03	3.7582E-04	1.0201E-04
		order	-	2.511	2.445
	$\gamma = 0.5$	e_h	6.3373E-04	1.4948E-04	4.2868E-05
		order	-	2.729	2.361
	$\gamma = 1.0$	e_h	1.4447E-03	3.3799E-04	1.0359E-04
		order	-	2.524	2.456
$\alpha = 0.9$	$\gamma = 0.0$	e_h	1.8541E-03	4.7506E-04	1.1826E-04
		order	-	2.063	2.106

Journal of http://www.satursonpublishing.com/
Research in Multidisciplinary Methods and Applications
ISSN 2957-3920 (Online) ISSN 3007-7060 (Print)
Volume 4, Issue 2, February 2025

	$\gamma = 0.5$	e_h	5.9003E-04	1.6085E-04	4.1629E-05
		order	-	1.969	2.048
	$\gamma = 1.0$	e_h	1.8740E-03	4.8283E-04	1.2039E-04
		order	-	2.054	2.104

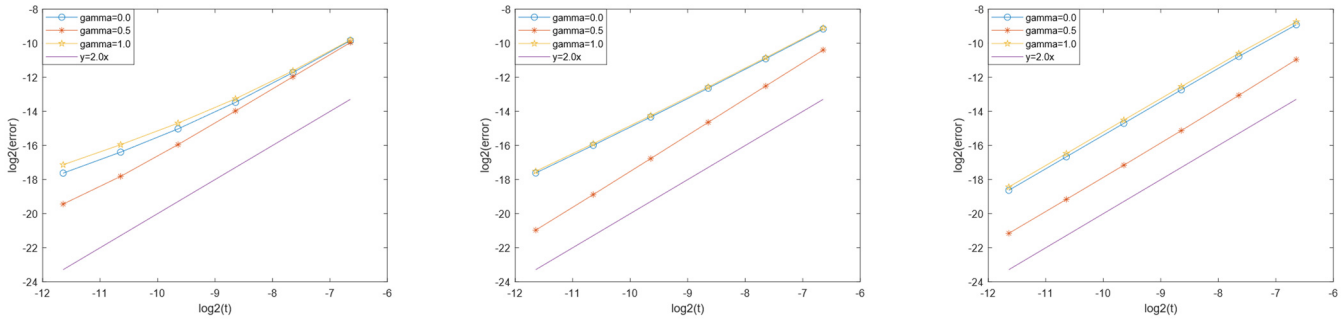

(A) $\alpha = 0.1$ **(B)** $\alpha = 0.5$ **(C)** $\alpha = 0.9$

FIGURE 4. THE PLOT OF TIME CONVERGENCE ORDER FOR EXAMPLE 2.

By Table 3 and Figure 3, we can find that our scheme tends to $1+\alpha$ in space. Furthermore, By Table 4 and Figure 4, it is clear that our scheme is of convergence second-order in time. These results once again verify the convergence order of this study.

Example 3. The Gaussian distribution is utilized to display the convection-diffusion movement. We take the domain $[a,b]=[-1,1]$, $V(x)=V_0(1-x)x$, where $V_0=1$. Let $K=0.3$, and the initial solution

$$u(x,0)=\mathrm{e}^{-\frac{(x-x_0)^2}{2\sigma^2}}. \tag{65}$$

In Figure 5, the movement of Gaussian peak with the different α and γ is given. When the two coefficients become bigger, the diffusion behavior over time is not significant. Figure 6 shows that when the weight γ becomes bigger, the left diffusion is more obvious at the same α. These results vividly illustrate the feasibility and effectiveness of this scheme in simulating convection-diffusion phenomena.

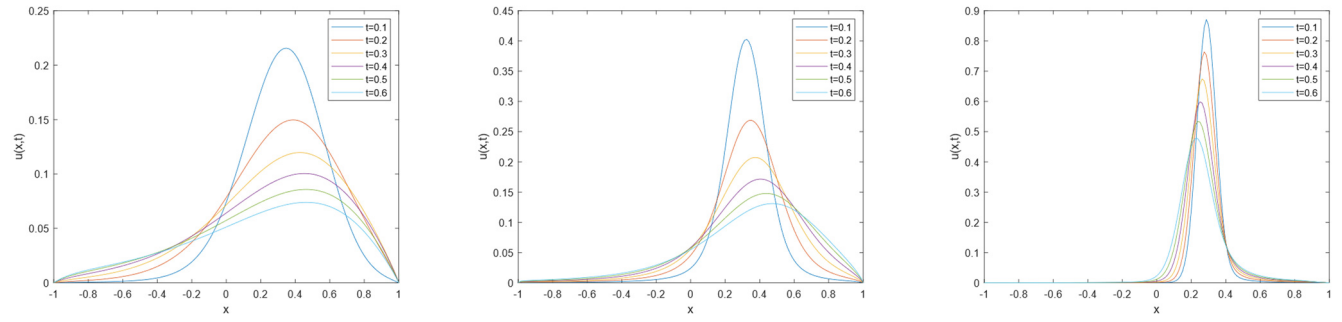

(A) $\alpha = \gamma = 0.1$ **(B)** $\alpha = \gamma = 0.5$ **(C)** $\alpha = \gamma = 0.9$

Journal of http://www.satursonpublishing.com/
Research in Multidisciplinary Methods and Applications
ISSN 2957-3920 (Online) ISSN 3007-7060 (Print)
Volume 4, Issue 2, February 2025

FIGURE 5. NUMERICAL SOLUTION AT DIFFERENT TIMES FOR EXAMPLE 3.

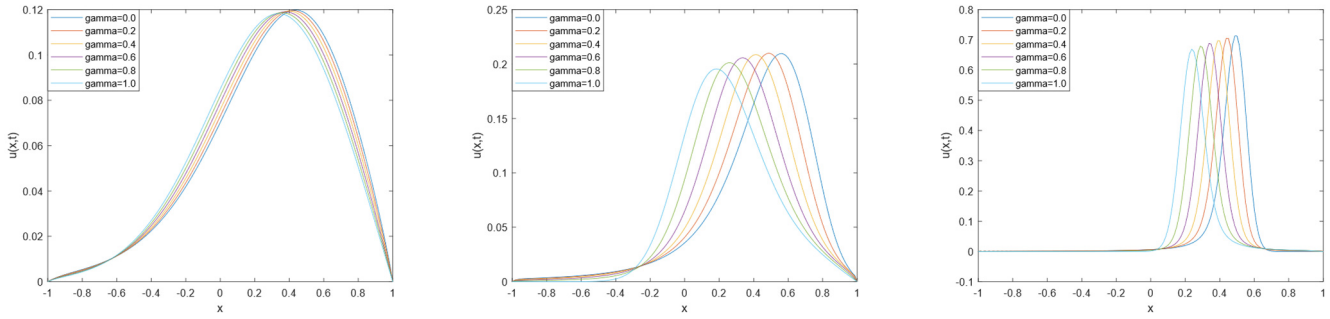

(A) $\alpha = 0.1$ **(B)** $\alpha = 0.5$ **(C)** $\alpha = 0.9$

FIGURE 6. NUMERICAL SOLUTION IN DIFFERENT PARAMETERS FOR EXAMPLE 3.

6 CONCLUSION

In this study, a time second-order characteristic finite volume method is successfully developed to address one-dimensional Riemann-Liouville space fractional convection-diffusion equations. By reformulating the original equation into a parabolic-like structure, the proposed method simplifies computational complexity while ensuring accuracy. A combination of the second-order Runge-Kutta method and the Crank-Nicholson implicit scheme demonstrates high efficiency and precision in temporal discretization, complemented by the spatial accuracy achieved through piecewise linear finite elements. Rigorous analysis confirmed the stability and convergence of the iterative coefficient matrix. Numerical experiments validate the theoretical convergence orders of $O(h^{1+\alpha})$ in space and $O(\tau^2)$ in time, and also illustrate our method's capacity in simulating the diffusion and convection behaviors under diverse parameter settings. The findings underscore the effectiveness and versatility of the proposed approach, making it a valuable contribution to the numerical study of fractional differential equations in applied sciences and engineering.

FUNDING

This study was supported by Beijing Natural Science Foundation (Grant No. 8232023) and Beijing Science and Technology Planning Project (Grant No. KM202111232009).

REFERENCES

[1] A. Bekir, "Exact solutions of some fractional differential equations arising in mathematical biology." International Journal of Biomathematics, 08 (2018): 155-203.

[2] B. Baeumer, D. Benson, M. Meerschaert, S. Wheatcraft, "Subordinated advection dispersion equation for contaminant transport." Water Resources Research, 37 (2001): 1543-1550.

[3] J. Kirchner, X. Feng, C. Neal, "Fractal stream chemistry and its implications for contaminant transport in catchments." Nature, 403 (2000): 524-526.

[4] R. Metzler and T. Nonnenmacher, "Fractional relaxation processes and fractional rheological models for the description of a class of viscoelastic materials." International Journal of Plasticity, 19 (2003): 941-959.

[5] R. Schumer, D. Benson, M. Meerschaert, B. Baeumer, "Multiscaling fractional advection dispersion equations and their solutions." Water Resources Research, 39 (2003): 1022-1032.

[6] X. Wang, M. Petru, L. Xia, "Modeling the dynamics behavior of flax fiber reinforced composite after water aging using a modified Huet-Sayegh viscoelastic model with fractional derivatives." Construction and building Materials, 290 (2021): 12-16.

[7] Y. Zhang and X. J. Yang, "An efficient analytical method for solving local fractional nonlinear PDEs arising in mathematical physics." Applied Mathematical Modelling, 40 (2015): 1793-1799.

[8] M. Chen and W. Deng, "Fourth order accurate scheme for the space fractional diffusion equations." SIAM Journal on Numerical Analysis, 52 (2014): 1418-1438.

[9] H. Ding, C. Li, Y. Chen, "High-order algorithms for Riesz derivative and their applications (II)." Journal of Computational Physics, 293 (2015): 218-237.

[10]T. Hang, Z. Zhou, H. Pan, Y. Wang, "The conservative characteristic difference method and analysis for solving two-sided space-fractional advection-diffusion equations." Numerical Algorithms, 92 (2023), 1723-1755.

[11]S. Vong, P. Lyu, X. Chen, et al., "High order finite difference method for time-space fractional differential equations with Caputo and Riemann-Liouville derivatives." Numerical Algorithms, 72 (2015): 195-210.

[12]W. Tian, H. Zhou, W. Deng, "A class of second order difference approximations for solving space fractional diffusion equations." Mathematics of Computation, 84 (2015): 1703-1727.

[13]L. Feng, P. Zhuang, F. Liu, I. Turner, Y. Gu, "Finite element method for space-time fractional diffusion equation." Numerical Algorithms, 72 (2016): 749-767.

[14]D. Nie, J. Sun, W. Deng, "Numerical algorithm for the model describing anomalous diffusion in expanding media." ESAIM Mathematical Modelling and Numerical Analysis, 54 (2020): 2265-2294.

[15]H. Wang and D. Yang, "Wellposedness of variable-coefficient conservative fractional elliptic differential equations." SIAM Journal on Numerical Analysis, 51 (2013), 1088-1107.

[16]J. Jia and H. Wang, "A preconditioned fast finite volume scheme for a fractional differential equation discretized on a locally refined composite mesh." Journal of Computational Physics, 299 (2015): 842-862.

[17]J. Jia and H. Wang, "A fast finite volume method for conservative space-fractional diffusion equations in convex domains." Journal of Computational Physics, 310 (2016): 63-84.

[18]F. Liu, P. Zhuang, I. Turner, K. Burrage, V. Anh, "A new fractional finite volume method for solving the fractional diffusion equation." Applied Mathematical Modelling, 38 (2014): 3871-3878.

[19]Aer. Simmons, Q. Yang, T. Moroney, "A finite volume method for two-sided fractional diffusion equations on non-uniform meshes." Journal of Computational Physics, 335 (2017): 747-759.

[20]J. Pan, M. Ng, H. Wang, "Fast preconditioned iterative methods for finite volume discretization of steady-state space-fractional diffusion equations." Numerical Algorithms, 74 (2017): 153-173.

[21]H. Fu, H. Liu, H. Wang, "A finite volume method for two-dimensional Riemann-Liouville space-fractional diffusion equation and its efficient implementation." Journal of Computational Physics, 388 (2019): 316-334.

[22]X. Zhang, J. Crawford, L. Deeks, M. Stutter, A. Bengough, I. Young, "A mass balance based numerical method for the fractional advection-dispersion equation: theory and application." Water resources research, 41 (2005): W07029.

[23]J. Douglas Jr. and T. Russell, "Numerical methods for convection-dominated diffusion problems based on combining the method of characteristics with finite element or finite difference procedures." SIAM Journal on Numerical Analysis, 19 (1982): 871-885.

[24]K. Wang and H. Wang, "A fast characteristic finite difference method for fractional advection-diffusion equations." Advances in water resources, 34 (2011): 810-816.

[25]H. Rui and M. Tabata, "A mass-conservative characteristic finite element scheme for convection-diffusion problems." Journal of Scientific Computing, 433 (2010): 416-432.

[26]P. Colella and P. Woodward, "The Piecewise Parabolic Method (PPM) for gas-dynamical simulations." Journal of computational physics, 54 (1984): 174-201.

[27]K. Fu and D. Liang, "The time second order mass conservative characteristic FDM for advection-diffusion equations in high dimensions." Journal of Scientific Computing, 73 (2017): 26-49.

[28]K. Fu and D. Liang, "The conservative characteristic FD methods for atmospheric aerosol transport problems." Journal of Computational Physics, 305 (2016): 494-520.

[29]K. Fu and D. Liang, "A mass-conservative temporal second order and spatial fourth order characteristic finite volume method for atmosphertic pollution advection diffusion problems." SIAM Journal on Scientific Computing, 41 (2019): 1178-1210.

[30]M. Celia, T. Russell, I. Herrera, R. Ewing, "An Euler-Lagrangian localized adjoint method for the advection-diffusion equations." Advances in water resources, 13 (1990): 187-206.

[31]H. Dahle, R. Ewing, T. Russell, "Eulerian-Lagrangian localized adjoint methods for a nonlinear advection-diffusion equation." Computer methods in applied mechanics and engineering, 122 (1995): 223-250.

[32]D. Liang, C. Du, H. Wang, "A fractional step ELLAM approach to high-dimensional convection-diffusion problems with forward particle tracking." Journal of Computational Physics, 221(2007): 198-225.